

Recurrent Neural Networks to Identify Fault in Transmission Line

Azriyenni Azhari Zakri*, Sahala Tua

Electrical Engineering Department, Universitas Riau-Pekanbaru, Indonesia
Email: azriyenni@eng.unri.ac.id



Abstract— The transmission system is the connecting part of the power station and, distribution is capable of being forwarded to the load center. If there is a fault in the transmission line by interrupting the electricity supply to the load, then this will cause a loss for consumers. Therefore, another technique is needed to identify the fault in the electrical power distribution system accurately and quickly by reducing search time and speeding up the repair process. This study will present a method to identify fault by classifying and estimating the location of a fault in the 115 kV transmission system. This technique is performed by combining Discrete Wavelet Transformation (DWT) and Recurrent Neural Networks (RNNs) of Elman. DWT aimed at extracting information of transient signals for each phase current and zero sequence current during one cycle when the fault starts. Elman RNNs are classified to detect a fault in each phase and ground, while Elman RNNs are used to measure the location of the fault in the transmission line. Training and testing data be carried out for the simulation of short circuit fault under different fault resistance and varying starting angle. Short circuit fault applied in the transmission line to 115 kV bus LK to BK on 63km line lengths. The fault classification results obtained are the accuracy of 100%, and the estimated location of fault received the most significant average error value is 1.4%.

Keywords— DWT, Elman RNNs, Fault Identification, Short-Circuit.

1. Introduction

The transmission line is an essential element of the electric power system to send electrical energy from a power station to a distribution network connected then to load. A fault that occurs in the transmission line can be converted to the termination of power supply in the distribution system, which gives rise to blackout at the consumer terminals [1]. The short-circuit fault may occur asymmetrically and symmetrically. Asymmetric fault comprises single-phase fault to ground, phase to phase, and second phases to ground. While symmetrical fault is the three-phase fault. Any kind of short-circuit fault that occurs has unique characteristics for current and voltage. However, any short-circuit fault that occurs on the transmission line must know about the type and how to address it differently. The application of Artificial Neural Networks (ANN) has been performed for the fault classification and the fault location in the transmission line. According to the results of Hessine's research that using modular ANN can shorten the duration of the training and improve the accuracy of ANN for the kinds of faults as well as estimating the fault location [2, 3]. It has also been proposed the application of DWT and SVM in order 4 using a sampling frequency of 50 kHz. Summing the absolute values of the detailed coefficients at levels 8 and 9 are used as input for SVM. The results obtained that this technique is applied parallel transmission line [4, 5]. This research will discuss the steps to class the faults and estimate the location of short circuit faults using the wavelet transformation and RNNs. The difference between wavelet transforms, and Fourier transforms that information is restricted only to the frequency domain. In contrast, information obtained by wavelet changes is in the form of frequency and time domains. DWT is a wavelet transform whose function is to receive information from transient signals when a short circuit fault begins [6].

A, A, Zakri et al. provided a backpropagation neural network to identify fault location in transmission line 150 kV among substation to substation. The fault in a power system is expended expanse relay protection equipment in the transmission line. Its requirements more growing big load, and grid systems are accumulative complexity. The protection system used digital control in order to avoid the error calculation of the distance relay impedance settings, and spent time will be more efficient. Afterward, backpropagation neural structure is a computational model that applies the training process that can be utilized to solve the problem of the work limitations of distance protection relays. The backpropagation neural network does not have boundaries cause of the impedance variety setting. If the output delivers the wrong result, so the correctness of the weight can be minimized and also the response of error, the backpropagation neural network is invented to be closer to the precise value. In the end, the backpropagation neural network demonstrating is asked to discover the fault location and identify operational output current circuit breaker was tripped it. The tests are implementation used system 150 kV of Riau region [2].

Otong et al. is presented to accurately detect a fault on the transmission line and quickly and reduce fault search time. The combination of the Park transformation method and the Adaptive Neuro-Fuzzy Inference System (ANFIS) can be observed at the distance of the fault location immediately post the fault. The technique used is a traveling wave analysis that changes current and voltage using the Park transformation at both ends of the line. The time difference at each line is justified by the fact that there is a difference in distance. This time difference will be imported to ANFIS to obtain the range of the fault location [7].

Neethu et al. have processed data generated by DWT to process transient signals as ANN input with backpropagation type. ANN technique with backpropagation type with TWD mother wavelet order dB4 of level 5 detail coefficients is more accurate to determine the type and location of the fault (A.S & T.S, 2017). Ahmed Saber et al. has proposed the application of DWT with a dB4 mother wavelet, a sampling frequency of 50 kHz wherein the implementation of the sampling frequency the values in one cycle are 1000 samples and SVM. Summing the absolute values of the element constants level 8 and 9 are used as SVM input. The results obtained that this method can classify disorders in parallel transmission lines correctly [8].

A. A, Zakri et al. implemented a hybrid method that is DWT and Support Vector Machine (SVM) for classification of fault in the transmission line. The DWT was set up to quotation the specified indication of transient D8 and D9 (order of 4) at 50 kHz for sample frequency. The value of Root Mean Square (RMS) will be given in the coefficients D8 and D9 for training and test data using the SVM technique. SVM is used to detect the fault every phase, and the ground is exposed in the kind of fault. The SVM method has been run consuming parameter C and kernel scale to accomplish the brilliant results of fault classification. The category of replicating fault has a difference of fault location, fault of resistance, and initial angle—the training and test data track for the test three bus systems [9].

Based on previous research relating to the identification of fault in the electric power transmission line using the concept of intelligent techniques. Identification of fault includes the classification and estimation of symmetrical short circuit fault. Then this research proposed a smart engineering concept using the DWT and RNN methods in the 115 kV transmission line. This model is expected to improve fault prediction by building a new Elman RNN structure. This research will be directed to excerpt D8 and D9 values consuming DWT with mother wavelet kind Daubechies (order of 4) at 50 kHz sample frequency. The targeted results of the models are predictable to accomplish the numerous precision of the fault classification.

2. Methodology

2.1 DWT

DWT has the capability to investigate several kinds of fault with info gotten rather than the frequency dominion and time dominion. The DWT is very valuable in discovering and dispensation numerous faults since of delicate to indication indiscretion [10]. The wavelet transform can be separated into two categories,

namely; DWT and Continuous Wavelet Transforms (CWT). The CWT is the number of indications overtime increased by the scale and position of the wavelet task, the equation [4, 9].

$$CWT(f, a, b) = \frac{1}{\sqrt{a}} \int_{-\infty}^{\infty} f(t) \varphi^* \left(\frac{t-b}{a} \right) dt \quad (1)$$

Discrete wavelet transforms considered as manageable implementations compared to continuous wavelet turns. The wave coefficient is obtained by applying DWT like the following equation [4, 9].

$$DWT(f, m, k) = \frac{1}{\sqrt{a_0^m}} \sum_k f(k) \varphi^* \left[\frac{n-ka_0^m}{a_0^m} \right] \quad (2)$$

CWT has several constants WT is a task as a measure and point. This stretches delivery to outcome numbers to be dismissed. The DWT has a couple of illustrations of WT of constants that were acquired of DWT to decrease the left-over of constants of CWT. DWT is employed to investigate wave indications proficiently and precisely. The DWT will be affected by a filter consuming Mallat procedure. DWT is separated into two wave indications that are; filter and downcast sampling processes. The high-pass clarify produces additional indications with great frequency. The low-pass sieves generate different indications with low frequency. After that, the figures will be achieved down the sampling process. So it only earnings half of every statistic acquired already [10, 11]. In Figure 1, we can indicate to the diagram of the sign dispensation by DWT. The extreme frequency signs are named elements and symbols with little frequencies named estimates. The procedure of decomposition by iteration consuming of guesstimate of the data gained formerly. It will be decayed to generate new approximation and feature records. Figure 2 expressions in the structure of the decay iteration procedure to become a further wave indication. It will be created by summing the calculation data and detail data [9, 12].

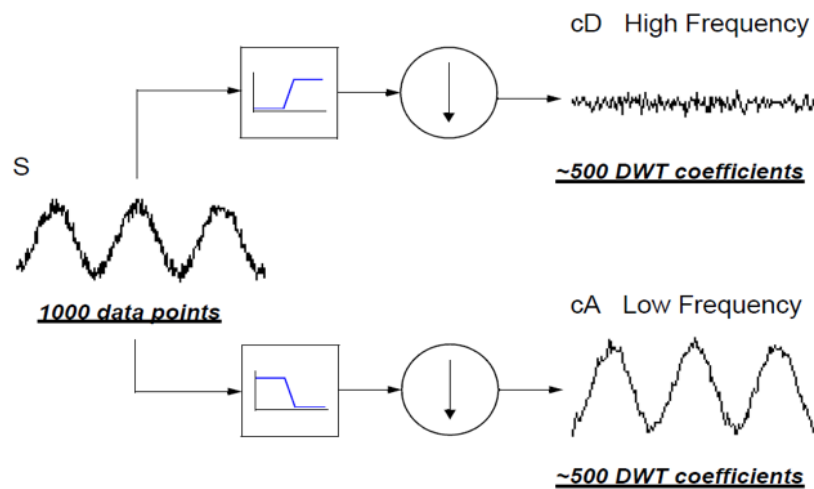


Fig. 1. Diagram signal processing DWT

a and b are scale constants and transition constants (time shifts), $CWT(f, a, b)$ is the coefficient of CWT and, φ is an artificial wavelet. Input signals have been rearranged using displacement and time expansion parameters for the right scale. In the wavelet transform, the mother wavelet is used in processing the original message. Mother wavelet consists of various types, such as; Haar, Daubechies, Coiflets, Symlets, etc. The most widely used mother wavelets are Daubechies, which are commonly composed DBN, somewhere N is the order, and DB shows the name of the Daubechies mother wavelet [9].

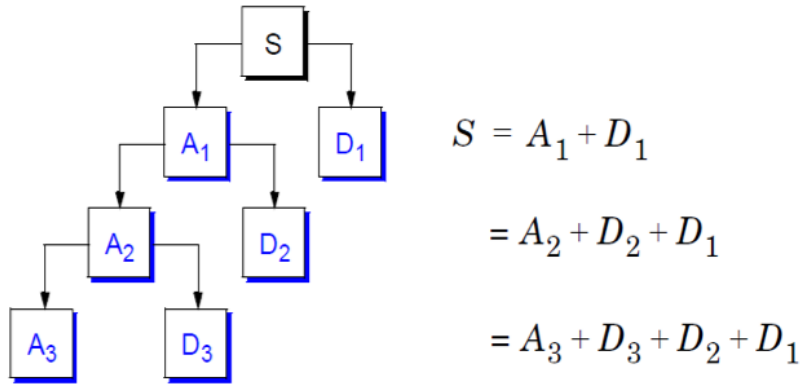


Fig. 2. The iteration is DWT decomposition

2.2 Elman RNNs Structure

A simple Recurrent Neural Network is a variation of the Multi-Layer Perceptron known as the Elman network, discovered by Jeff Elman. The main difference structure is that; there are units adjacent to the input layer that is attached to the hidden layer. The group includes the contents of one of the layers that existed when the previous pattern was trained. Elman RNNs involves one or more hidden layers. The first layer has the weight obtained from the input layer. Each layer will receive the weight since the first layer. This structure customs initiation purposes recognized as binary sigmoid, bipolar sigmoid for hidden input layer, and a linear role for the output layer [2, 4].

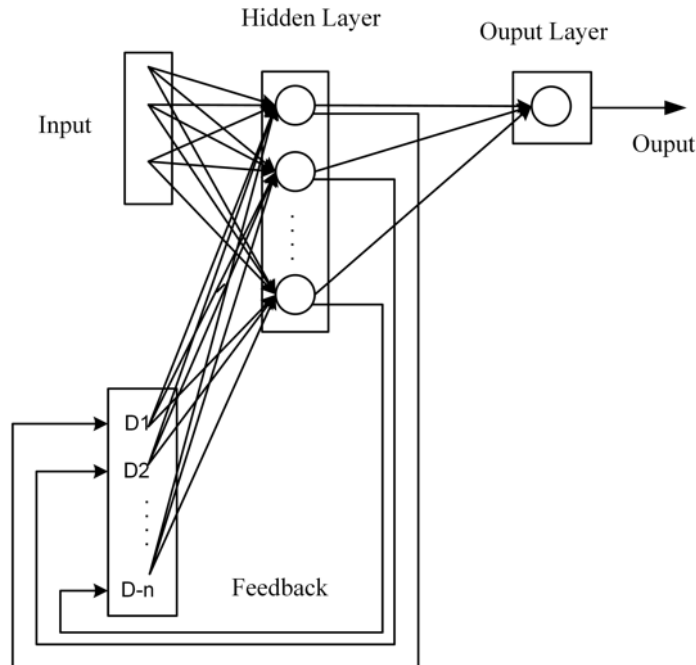


Figure 3. Structure of Elman RNNs

This Elman network has a triggering role that can have some function, both continuous and discontinuous. The delay that occurs in the relationship among the input layer and the first hidden layer in the prior time (t-1) can be utilized to know (t). Figure 3 is the Elman RNNs structure having a feedback connection

consisting of disturbance information on the previous input to be accommodated for the data. The nature of this feedback is that the unit can still be recycled information through the network for some time and thus find an abstract representation of time. RNNs have activation feedback embodying short-term memory. The layer is refreshed not only by external network input but also by activation of prior forward propagation. This response is replaced with a set of weights to allow reflex adaptation [10].

2.3 Power System Transmission

Figure 4 is the transmission system expanded is collected from three buses that are; Bus LK to Bus BK. The transmission line system is presently below a voltage of 115 kV besides a frequency of 50 Hz. In the transmission line among the Bus LK and the Bus BK at short-circuit fault. The interval of a transmission line from Bus LK to Bus BK is 63km.

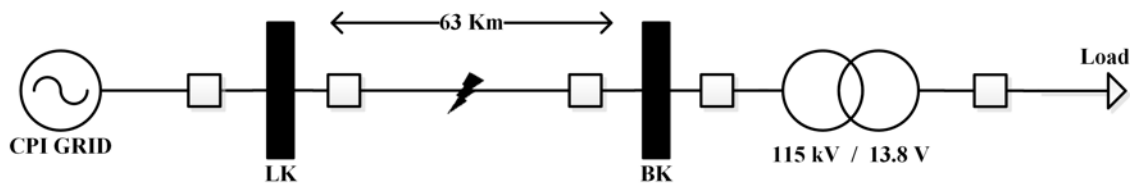


Fig. 4. Single line diagram transmission system

Fault current obtained by simulation results using a 50 kHz sampling frequency is processed using the DWT function. Flow is observed during one cycle after the fault occurs. The fault current is processed using DWT after the DWT output becomes input data for Elman RNNs to determine the classification and estimation of fault locations. The sequence of wavelet decay with a sampling frequency of 50 kHz can be seen in Table 1. The more decomposition process, the sign can be separated into several low-resolution components. Accordingly, the lower frequency component filter process will be run continuously. Table 1 designates the decomposition of wavelet level 9 for a single cycle after the fault with a sampling frequency of 50 kHz [9, 11].

Table 1. The wavelet decomposition command

Level	Approximation	Detail
1	0 – 12.5 kHz	12.5 – 25 kHz
2	0 – 6.25 kHz	6.25 – 12.5 kHz
3	0 – 3.125 kHz	3.125 – 6.25 kHz
4	0 – 1.563 kHz	1.563 – 3.125 kHz
5	0 – 781 Hz	781 – 1.563 kHz
6	0 – 391 Hz	391 – 781 Hz
7	0 – 195 Hz	195 – 391 Hz
8	0 – 98 Hz	98 – 195 Hz
9	0 – 49 Hz	49 – 98 Hz

The selection of the best Elman RNN structure of results in the classification Elman RNNs kind and estimated of fault location. Then the Elman RNNs test was selected with different input from the training and testing data, as indicated in Table 2. Accuracy and error obtained from the Elman RNN classification results and the estimated fault location has been selected.

Table 2. Parameters for testing RNNs of the classification and estimation of fault locations

Identification	Fault	L (%)	R (Ω)	D ($^{\circ}$)
Classification & Estimated fault	LG	1,6, 5,6, 9,6, ..., 93,6, 97.6	45	65
	LL			
	LLG			
	LLL			

2.4 RNNs of Elman for Fault Classification

RNNs is manufactured using the Elman networks, which classifies fault in each phase and ground that work in parallel. When there is a fault in a phase, then the Elman RNNs will provide information on the form of fault in that phase. If there is a fault of the ground, the RNNs will be delivered through the zero-sequence current signal and given the information of the fault according to the zero-sequence current values that are trained on the Elman RNNs. Figure 5 shows all the data from the fault classification, and it is known that a short circuit fault happens on the transmission line.

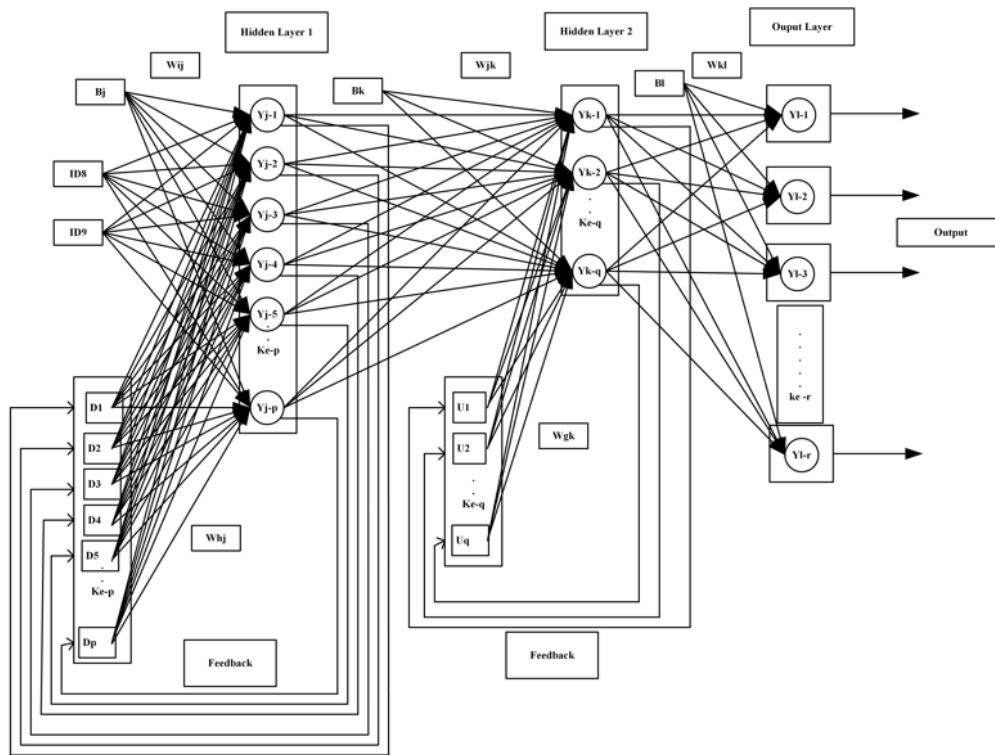


Figure 5. Elman’s RNN Structure of fault classification

Figure 5 is further the structure of RNNs consisting of input data, hidden layers, and output layers. The output appears in the form of whether or not there is a fault with the phase and ground. In the Elman RNNs simulation, the fault given is variations in the current RMS values for the coefficients D8 and D9. Input variations can be divided into [13]:

- 2 RMS phase current details coefficients A

- 2 RMS phase current details coefficients B
- 2 RMS phase current details coefficients C
- 2 RMS coefficients details of the zero-sequence current

For each RNNs classifies the fault in phase A, B, and C that is used as input is a sample of the fault current in each phase. Classification of fault on the ground serves as a zero-sequence current input.

2.5 RNNs of Elman for Fault Estimation

Elman RNNs estimated the location of fault was built to determine the location of a fault in each fault and provide the results of fault at the distant location. Each type of fault is under RNNs structure for estimating different fault locations. Types of fault that has been simulated are LG (AG, BG, CG), LL (AB, AC, BC), LLG (ABG, ACG, BCG) and LLL (ABC) fault. In designing Elman RNNs for estimating the location of this fault, it will be finished with input variations. In this RNNs, two structures are integrated into; RNNs 1 and RNNs 2. The difference in the value of I_{r_dec} RNN 1 is 0.6, and the amount of I_r of RNN 2 is 0.7. This intends to choose the results of accuracy and duration of training that is better and faster for training the estimated location of a fault. Figure 6 shows the training process carried out 100 times. Iteration with training error tolerance value is 0.000001. Elman RNN structure for fault estimation.

Figure 6 is Elman's RNN structure for estimating fault locations. The RNN was constructed to estimate the location of the fault consisting of input data, hidden layer, and output layer. The resulting output data are information in the form of distance to the location of the fault. For the estimated location of the fault, six input data are given, namely the RMS current coefficient D8 and D9 after each phase fault, as formulated as follows [11, 13]:

$$X_{FL} = [ID8_A, ID9_A, ID8_B, ID9_B, ID8_C, ID9_C] \quad (3)$$

X_{FL} : Input RNN for estimated fault location, $ID8_i$: RMS current for D8 coefficient post fault, $ID9_i$: RMS current for current D9 coefficient post fault, i : Phase A, B, C.

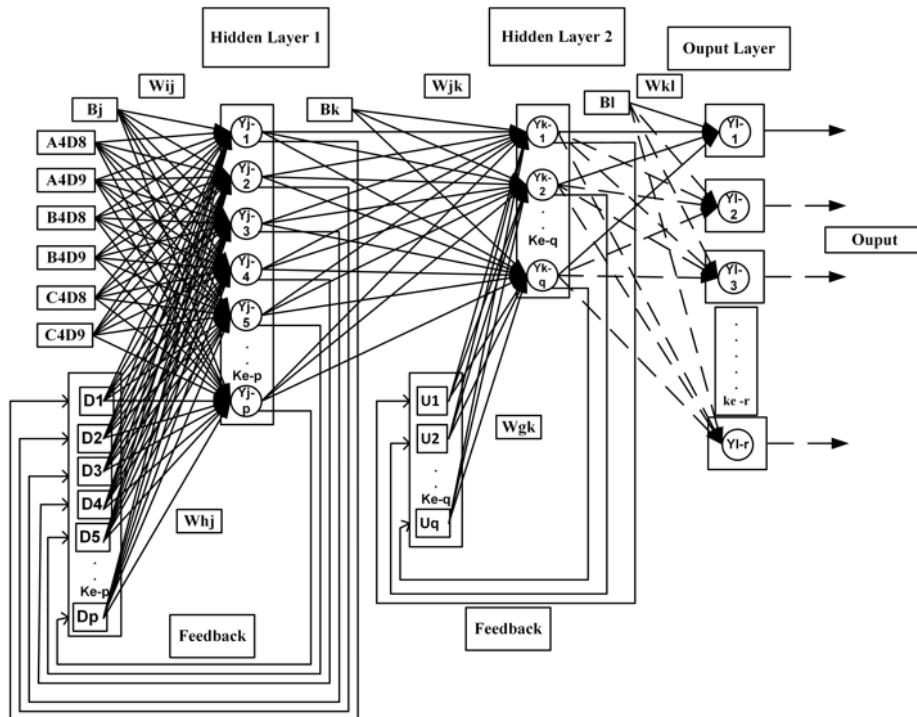


Figure 6. Elman RNN structure estimated fault location

2.6 Mean Absolute Percentage Error (MAPE)

To validate the reliability of a forecast process, you can use MAPE. How to get the MAPE consists of calculating the absolute error of each period divided into the actual observation value for that period. MAPE calculation results are used to determine whether or not the predictions produced. Predictive ability is beneficial if the MAPE is less than 10%, y_i : target value, y'_i : predictive output, n : the amount of data [5, 9].

$$\text{MAPE} = \frac{\sum \frac{|y_i - y'_i|}{y_i}}{n} \times 100\% \quad (4)$$

3. Results

Training for estimated fault locations for RNN 1 was carried out as much as 38,669 iterations on the duration of 3 minutes 4 seconds. When RNN 2 runs 7212 iterations at a term of 24 seconds. Then, testing for the Elman RNN structure was trained to estimate the location of the fault when ABC fault occurred. Testing for the assessed area of RNN 1 fault has an iteration of 500,000 with a training duration of 3 hours 42 minutes 4 seconds. Furthermore, RNN 2 is executed with 325,191 iterations in the period of the training 1 hour 23 minutes 39 seconds. After conducting training and testing on various types of Elman RNN classification and estimation of fault locations, the outputs of each network are then seen. The Elman RNN is used based on the production of the Elman RNN, namely by looking at the smallest MAPE value and training duration in the classification and estimation of the fault location of each Elman RNN. The results of the Elman's RNN structure selection used are as shown in Table 3.

Table 3. Elman RNNs structures used for classification and estimated of fault location

Elman RNN Structures	Elman RNN Structures
Fault Classification of Phase A	A1D8 – A10D8, A1D9 – A10D9
Fault Classification of Phase B	B1D8 – B10D8, B1D9 – B10D9
Fault Classification of Phase C	C1D8 – C10D8, C1D9 – C10D9
Fault Classification of Ground	N1D8 – N10D8, N1D9 – N10D9
Estimated Location of Fault AG	A1D8, A1D9, B1D8, B1D9, C1D8, C1D9
Estimated Location of Fault BG	A2D8, A2D9, B2D8, B2D9, C2D8, C2D9
Estimated Location of Fault CG	A3D8, A3D9, B3D8, B3D9, C3D8, C3D9
Estimated Location of Fault AB	A4D8, A4D9, B4D8, B4D9, C4D8, C4D9
Estimated Location of Fault AC	A5D8, A5D9, B5D8, B5D9, C5D8, C5D9
Estimated Location of Fault BC	A6D8, A6D9, B6D8, B6D9, C6D8, C6D9
Estimated Location of Fault ABG	A7D8, A7D9, B7D8, B7D9, C7D8, C7D9
Estimated Location of Fault ACG	A8D8, A8D9, B8D8, B8D9, C8D8, C8D9
Estimated Location of Fault BCG	A9D8, A9D9, B9D8, B9D9, C9D8, C9D9
Estimated Location of Fault ABC	A10D8, A10D9, B10D8, B10D9, C10D8, C10D9

The DWT output is used as input to Elman's RNN. The training process is carried out with a maximum iteration of 500,000 with a tolerance value of 0.0001. The two RNN structures are; structure one uses the gradient descent adaptive learning rate for RNN 1 and, the second structure uses the gradient descent adaptive learning rate for RNN 2. Table 5 shows the structure of RNN 1 built on the standard gradient descent adaptive learning rate. At the same time, RNN 2 is a standard gradient descent adaptive learning rate aimed at reducing the duration of training. The different parameters of RNN 1 and RNN 2 are detailed in that table. Table 6 shows the simulation results for the classification of fault determined that there is a fault in each phase and ground correctly according to the type of fault that occurs. Hence, the accuracy of the fault classification is

100%. The simulation of the fault location estimated using MAPE with minimal value. Each type of fault produced an excellent error value, namely, 1,017433% for RNNs 1 and 1,418568% for RNNs 2.

Table 5. Elman's RNN parameters classification and estimated fault location

Characteristic	RNN 1	RNN 2
Architecture	two hidden layer	two hidden layer
Neuron input	fault current of D8 & D9	fault current of D8 & D9
Neuron hidden layer 1	48	48
Neuron hidden layer 2	24	24
Neuron output	1	1
The activation function of hidden layer 1	Sigmoid binary	Sigmoid binary
The activation function of hidden layer 2	Sigmoid bipolar	Sigmoid bipolar
The activation function of the output layer	linear function	linear function
Weight	Min Max	Min Max
Toleransi error	0.0001	0.0001
Maximum iteration	500,000	500,000
Learning rate	0.1	0.1
Ratio to increase the learning rate	1.05	1.05
Ratio to decrease the learning rate	0.6	0.7
The maximum increase in performance	1.06	1.06

Table 6. MAPE of Elman's RNN 1 & 2 are used to identify the fault

Fault	Error (%)					
	MAPE		Maximum		Minimum	
	RNNs 1	RNNs 2	RNNs 1	RNNs 2	RNNs 1	RNNs 2
AG	0.245137	0.245137	0.241118	0.241118	0.000029	0.000029
BG	0.504459	0.622443	0.378000	0.281476	0.004000	0.281476
CG	0.321504	0.328350	0.207000	0.264986	0.000000	0.264986
AB	0.282843	0.680925	0.261000	0.412825	0.000000	0.000929
AC	0.892839	0.892839	0.306349	0.306349	0.006151	0.006151
BC	1.017433	0.386365	0.362200	0.202113	0.002000	0.000795
ABG	0.605522	1.418568	0.250963	0.430777	0.000912	0.006889
ACG	0.326534	0.326534	0.305512	0.305512	0.001058	0.001058
BCG	0.502179	0.502179	0.305233	0.305233	0.002017	0.002017
ABC	0.629717	0.629717	0.270158	0.270158	0.004765	0.004765

4. Conclusion

Based on the Elman RNN networks design as fault classified and estimated fault location in the 115 kV transmission system. It is concluded that the Elman RNN for fault classification is carried out for each phase and soil correctly and following the type of fault so that the accuracy of Elman RNN for fault classification is 100%. Then, the average error value for Elman RNN structure testing for the estimated fault location of 0.245137% occurred in the type of fault AG (RNNs 1 & 2). When the most significant average error generated for the estimated location of the fault (BC) is 1.017433% (RNNs 1 & 2). So that from all analyzes obtained the error results below 10%, it can be possible to conclude that the category of fault prediction using Elman's RNN networks is very good at determining the predicted fault in the 115 kV transmission line.

Acknowledgment

The author would like to thank the Ministry of Research, Technology, and Higher Education (RISTEKDIKTI), Republic of Indonesia.

References

- [1] Sofianos, N.A. and Y.S. Boutalis, Stable Indirect Adaptive Switching Control for Fuzzy Dynamic System Based on T-S Multiple Models. *International Journal of Systems Science*, 2013. **44**(8): p. 1546-1565.
- [2] Azriyenni, M.M., DY Sukma, ME Dame, Backpropagation Neural Network Modeling for Fault Location in Transmission Line 150 kV. *Indonesian Journal of Electrical Engineering and Informatics (IJEI)*, 2014. **2**(1): p. 1-12.
- [3] Azriyenni and M.W.Mustafa, Application of ANFIS for Distance Relay Protection in Transmission Line. *International Journal of Electrical and Computer Engineering (IJECE)*, 2015. **5**(6): p. 1311-1318.
- [4] Mosavi, M., Tabatabai, A, Wavelet, and neural network-based fault location in power systems using statistical analysis of traveling waves. *Arab J Sci Eng*, 2014: p. 1-8.
- [5] Reddy, M.J. and D.K. Mohanta, Adaptive-neuro-fuzzy inference system approach for transmission line fault classification and location incorporating effects of power swings. *IET Generation, Transmission & Distribution*, 2008. **2**(2): p. 235. *IET Generation, Transmission & Distribution*, 2008. **2**(2): p. 235.
- [6] K. Chen, C.H., J. He, Fault detection, classification and location for transmission lines and distribution system: a review on the methods. *High Voltage*, 2016. **1**(1): p. 25-33.
- [7] Otong, M., Alimuddin, B, C. A, Deteksi Jarak Lokasi Gangguan Pada Saluran Transmisi 500 Kv Cilegon Baru - Cibinong Menggunakan Adaptive Neuro-Fuzzy Inference System (ANFIS). 2017.
- [8] Saber, A., Emam, A., & Amer, R, Discrete Wavelet Transform and Support Vector Machine Based Parallel Transmission Line Fault Classification. *IEEE Transactions on Electrical and Electronic Engineering*, 2016: p. 43-48.
- [9] Azriyenni Azhari Zakri, S.D., Jafaru Usman, Iswadi Hasyim Rosma, Boy Ihsan, Extract Fault Signal Via DWT and Penetration of SVM for Fault Classification at Power System Transmission. *IEEE*, 2018: p. 191-196.
- [10] M. Misiti, G.O., J.-M. Poggi, *Wavelet Toolbox™ Getting Started Guide*. 2016, Natick: The MathWorks, Inc.
- [11] A. A. M. Zin, M.S., M. W. Mustafa, A. R. Sultan, Rahimuddin, New algorithm for detection and fault classification on a parallel transmission line using DWT and BPNN based on Clarke's transformation. *Neurocomputing*, 2015. **168**(30): p. 983-993.
- [12] Addison, P.S., *The Illustrated Wavelet Transform Handbook: Introductory Theory and Applications in Science, Engineering, Medicine, and Finance*. 2017, CRC Press.
- [13] He, Z., *Wavelet Analysis and Transient Signal Processing Applications for Power Systems*. 2016: Wiley.



This work is licensed under a Creative Commons Attribution Non-Commercial 4.0 International License.